Sensors and Actuators B 242 (2017) 1115–1120

Contents lists available at ScienceDirect

Sensors and Actuators B: Chemical

journal homepage: www.elsevier.com/locate/snb

Integrated humidity sensor based on SU-8 polymer microdisk microresonator

M. Eryürek[a], Z. Tasdemir[d], Y. Karadag[b], S. Anand[a], N. Kilinc[c], B.E. Alaca[d,e], A. Kiraz[a,f,*]

[a] Department of Physics, Koç University, Rumelifeneri Yolu, 34450 Sariyer, Istanbul, Turkey
[b] Department of Physics, Marmara University, 34722 Goztepe, Istanbul, Turkey
[c] Mechatronics Engineering Department, Nigde University, 51245 Nigde, Turkey
[d] Department of Mechanical Engineering, Koç University, Rumelifeneri Yolu, 34450 Sariyer, Istanbul, Turkey
[e] Surface Science and Technology Center, Koç University, Rumelifeneri Yolu, 34450 Sariyer, Istanbul, Turkey
[f] Department of Electrical and Electronics Engineering, Koç University, Rumelifeneri Yolu, 34450 Sariyer, Istanbul, Turkey

ARTICLE INFO

Article history:
Received 2 May 2016
Received in revised form 27 July 2016
Accepted 22 September 2016
Available online 25 September 2016

Keywords:
Microdisk
Whispering gallery mode
SU-8
FEM
humidity sensor
microresonator

ABSTRACT

Due to its high interaction with water vapor and photolithographic patterning property, SU-8 is a favorable hygroscopic polymer for developing humidity sensors. In addition, optical resonances of optical microresonators are very sensitive to the changes in their environment. Here, we present integrated optical humidity sensors based on chips containing SU-8 polymer microdisks and waveguides fabricated by single-step UV photolithography. The performance of these sensors is tested under a wide range of relative humidity (RH) levels (0–50%). A tunable laser light is coupled from an excitation fiber to individual SU-8 waveguides using end-face coupling method. As the laser wavelength is scanned, the whispering gallery modes (WGMs) are revealed as dips in the transmission spectra. Sensing is achieved by recording spectral shifts of the WGMs of the microdisk microresonators. Red shift is observed in the WGMs with increasing RH. Between 0 and 1% RH, an average spectral shift sensitivity of 108 pm/% RH is demonstrated from measurements performed on 4 sensor devices. This sensitivity is comparable to the highest values obtained using microresonators in the literature. Measurements performed with another sensor device revealed a decrease in sensitivity by only around 3 times when RH is increased to 45–50%. Finite element modeling simulations are carried out to determine the dominant effect responsible for the resonance shift. The results show that the refractive index change is more important than the microresonator size change. The standard deviation in wavelength measurement is <3 pm, indicating a limit of detection better than 0.03% RH. These results suggest that optical sensor devices that contain integrated SU-8 microresonators and waveguides can be employed as easy-to-fabricate and sensitive humidity sensors.

1. Introduction

Detection of very small changes in relative humidity (RH) is desirable for a wide range of applications including textile processing, automotive industry, agriculture, food preparation, preservation of archeological samples, photoresist production, Si wafer processing, and production of electrical components [1,2]. Industrial processing, environmental control and pharmaceutical processing also require precise RH monitoring for better quality products [3]. Therefore there is a tremendous effort towards building humidity sensors [3] employing different sensing mechanisms which include capacitive [4], resistive [5], hygrometric [6], gravimetric [7] and optical [8] technologies. Capacitive and resistive methods are low cost, mass producible and have a wide dynamic range, but they are not reliable at RH levels under 5% [2]. Hygrometric and gravimetric methods have low hysteresis and drift, but hygrometric sensors have high uncertainty in measurement and gravimetric sensors require relatively complicated systems for signal processing [2]. In contrast, optical sensors are smaller, more sensitive, more flexible, and they can operate under harsh environments, such as under the presence of other chemicals or RF noise from electromagnetic interference [2]. Optical sensors mostly rely on monitoring the optical intensity changes [9,10], which can be affected by the internal intensity fluctuations of the light source. Avoiding such measurement errors is possible through spectroscopic measurements of the optical resonances of microresonators. Optical microresonators with high quality factors have been employed in many applications for

* Corresponding author.
E-mail address: akiraz@ku.edu.tr (A. Kiraz).

http://dx.doi.org/10.1016/j.snb.2016.09.136
0925-4005/

sensitive chemical or biological detection [11,12]. However, to date only a few reports have demonstrated RH detection using microresonators [13–17]. These demonstrations have employed silica microspheres coated with SiO_2 nanoparticles [13], polymer SU-8 microrings coated with a sol-gel thin film [14], silica microtoroids coated with a humidity responsive polymer [15], rolled polymer/oxide/polymer nanomembranes [16] and microfiber knot resonators [17]. Whispering gallery modes (WGMs) exhibited spectral drifts with sensitivities of ~4, 16, 10–13, 130 and ~9 pm/% RH, in [13–17], respectively.

In this work, we present an RH sensor using an SU-8 polymer optical microdisk microresonator. SU-8 is a very good material for optical RH sensing because of its high refractive index (1.57 at 1550 nm) [18] and low absorption (>95% transmission at 1550 nm [19]), good mechanical stability [20] and high interaction with water vapor, i.e. hygroscopic nature [21]. Between 0 and 1% RH, we achieve an average detection sensitivity of 108 pm/% RH, almost one order of magnitude higher than four of the previous demonstrations [13–15,17], and comparable to the other work, which, however, requires more complicated fabrication and sample preparation steps [16]. Our measurements also show good sensor response for RH values up to 50%. Our sensor devices that include optical waveguides and microdisk microresonators are fabricated with standard single-step UV photolithography. In the presence of water vapor, refractive index change and radius change of the microresonator can give rise to the spectral shifts of the WGMs. Previous microresonator-based RH sensors were shown to employ only refractive index change [13,14,17] or only radius change [16]. One study took advantage of both phenomena [15], but their respective contributions to the sensing signal were not elaborated. In our work, we incorporate detailed finite element modeling (FEM) simulations to determine the contributions from refractive index and radius changes. Our analysis shows that, refractive index change is the dominant mechanism governing the operation of our sensors. Further sensor properties such as sensitivity, hysteresis, analysis of response and recovery and repeatability are also investigated.

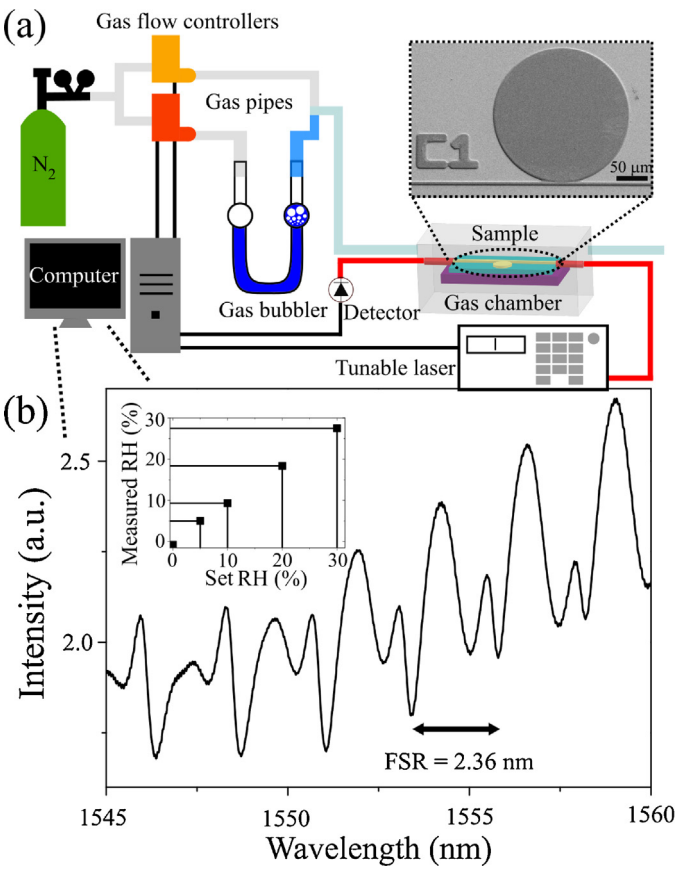

Fig. 1. (a) Experimental setup used for humidity sensing experiments. One exemplary transmission spectrum is given in (b). An SEM image of the microdisk is given as an inset. The inset in the transmission spectrum shows the measured RH values from the commercial humidity sensor as a function of the RH values set using the gas flow controllers.

2. Fabrication of microdisk resonators

In comparison to microspheres or microtoroids, microdisks possess WGMs with relatively low quality factors [11]. This hampers the performance of optical sensors using microdisks. Despite this fact, in this work, SU-8 microdisks are selected as the optical microresonators of choice due their ease of fabrication. Standard single-step UV photolithography is used to obtain optical sensors containing microdisks and optical waveguides in the form of integrated chips. These sensor devices are robust and suitable for point-of-care measurements. In addition, they do not necessitate additional fragile components such as optical fiber tapers [22] for their operation. Microdisk RH sensor consists of an integrated pair of microdisk and waveguide, both made out of SU-8 on a 4-inch commercial ⟨100⟩ Si wafer (wafer thickness is 500–550 μm, resistivity: <0.05 Ωcm). The wafer incorporates a 5-μm-thick thermal-oxide layer with the index of refraction lower than that of SU-8 to ensure light guiding inside SU-8 layer. Fabrication of the sensor device is carried out using standard UV photolithography. SU-8 2002 is spin coated on the wafer with a two-step spin coating recipe: 500 rpm for 10 s and 3000 rpm for 60 s. The waveguides are 2–3 μm wide, the radius of the microdisk is 100 μm and their thickness is 1.5–2 μm. Microfabrication is completed with soft bake (1 min), exposure, post-exposure bake (PEB, 2 min) and development steps. Both soft bake and PEB are performed at 95 °C. The wafer is then cut along cleavage planes to obtain sample chips. This allows having smooth waveguide cross sections at the chip edges to minimize losses during the end-face coupling. An electron microscope image of a sample sensor device is shown as an inset in Fig. 1(a). More than 100 sensor devices have been fabricated with the same geometrical parameters. More than 10 of these devices have been tested. Detailed sensor characterization experiments performed on 5 of these sensors devices are reported in this manuscript.

3. Experimental setup

Once the sensor chips are fabricated, they are placed in a small gas chamber (dimensions are $10 \times 23 \times 38\ mm^3$) for testing their humidity sensing performance (see Fig. 1(a)). Two arms of nitrogen gas (N_2) are used to control RH level in the chamber. N_2 from the first arm is sent directly into the gas chamber, whereas the second N_2 arm is sent through a gas bubbler containing DI water. N_2 flow rates of both arms are controlled by gas flow controllers (Bronkhorst, F-201CV, accuracy: ±(0.5% Rd + 0.1%FS)) so as to obtain the desired RH value in the chamber. The RH values set by the flow controllers are independently verified using a commercial humidity sensor (Honeywell, HIH-4010-003, accuracy: ±3.5%, repeatability: ±0.5%). Inset in Fig. 1(b) shows the RH values measured with the commercial sensor as a function of those set with the flow controllers. Considering the ±3.5% accuracy of the commercial sensor, a good match is obtained between the measured and set valued. At the beginning of each experiment, the gas chamber is purged with N_2 (purity 99.995%) for 1.5–2 h in order to make sure that the RH level is 0%. Tunable laser light (tuning range:

1500–1620 nm) is coupled from a single mode optical fiber to the SU-8 waveguide using end-face coupling [23]. The transmission signal is collected with a photodiode placed at the end of a single mode optical fiber coupled to the other end of the SU-8 waveguide. Microdisk WGMs are observed as dips in the transmission signal recorded as a function of the laser wavelength. As the RH is increased, red-shift is observed in the WGMs present in consecutive transmission spectra. This spectral shift ($\Delta\lambda$) is ultimately used as the sensing signal. An exemplary transmission spectrum is given as an inset in Fig. 1(b). From this spectrum, the free spectral range (FSR) is determined as 2.36 nm. This value is in a good agreement with the previous similar studies [24,25] and the calculated FSR of 2.45 nm for a 100 μm radius SU-8 microdisk around 1555 nm.

4. Spectral shift mechanisms

Refractive index change (Δn) and radius change (ΔR) are two mechanisms that give rise to $\Delta\lambda$. The relation between $\Delta\lambda$, Δn and ΔR is given by [14–16]:

$$\frac{\Delta\lambda}{\lambda} = \frac{\Delta n}{n} + \frac{\Delta R}{R} \quad (1)$$

where λ, R and n correspond to initial wavelength, radius and refractive index, respectively. In order to determine $\Delta R/R$, FEM simulations are carried out using a commercial FEM software package. SU-8 microdisks having a radius of 100 μm and a thickness of 1.5 μm are simulated for two cases: (1) Free-standing microdisk which can displace freely in the radial direction to compare with the analytical solution. (2) Microdisk on an infinitely rigid support to compare with the experimental results. For the two studied cases, radial displacement, u, is obtained as a function of radial distance, r (see Fig. 2).

Microdisk deformations are modeled by considering the humidity expansion coefficient (HEC) of SU-8 at room temperature to be equal to 25.3 ppm/% RH [21]. To the best of our knowledge, Ref. [21] is the only study mentioning the HEC of SU-8, but a similar value (18 ppm/% RH) is reported for another hygroscopic polymer, tert-butylcalix[6]arene (TBC6A) [26]. Utilizing the analogy with thermal strains, HEC is introduced into the FEM to account for expansions as a result of humidity. All simulations are carried out for an RH value of 1%. A linear elastic material model is utilized together with built-in SU-8 mechanical material properties and all simulations are carried out in 3D. For the simulations, tetrahedral and triangular elements are employed with minimum mesh element numbers of 12×10^4 and 22×10^3 for tetrahedral and triangular element types, respectively. The number of degrees of freedom solved is around 10^6. The expansion of the microdisk is obtained at three different locations along the bottom surface, mid-plane and the upper surface of the microdisk.

Fig. 2(a) shows the displacement of the mechanically unrestrained microdisk. For this geometry, the displacement values obtained from FEM simulations show excellent agreement with the analytical formula:

$$u = (r)(HEC) \quad (2)$$

Once the model is verified with the analytical solution, restrained disk case is studied which corresponds to the experimental measurements in this work, *i. e*. SU-8 microdisk mechanically fixed from its bottom boundary surface (see Fig. 2(b)). Since the expansion of the microdisk is mechanically constrained, maximum radial expansion is only 0.08 nm at the outer circumference. This value is 0.06 nm when the middle plane in the vertical direction is considered. Using the result from the middle plane, $\Delta R/R$ value is found to be 6×10^{-7}/% RH, which is almost two orders of magnitude less than the observed average $\Delta\lambda/\lambda \sim 7 \times 10^{-5}$/% RH. Therefore we conclude that the contribution of $\Delta R/R$ to $\Delta\lambda/\lambda$ is negligible.

5. Results and discussion

For sensitivity characterizations four different SU-8 microdisk microresonator-based sensors are tested under various RH values from 0% to 7% (see Fig. 3). Consecutive WGM spectra are recorded and spectral shifts of the WGM are analyzed with a Lorentzian fitting code. These sensors have the same design geometry, but they are fabricated at different locations on the wafer. For Sensor 1, the WGM used in the RH measurements is at around 1529.74 nm with Q factor of about 10^3 before water vapor is introduced into the

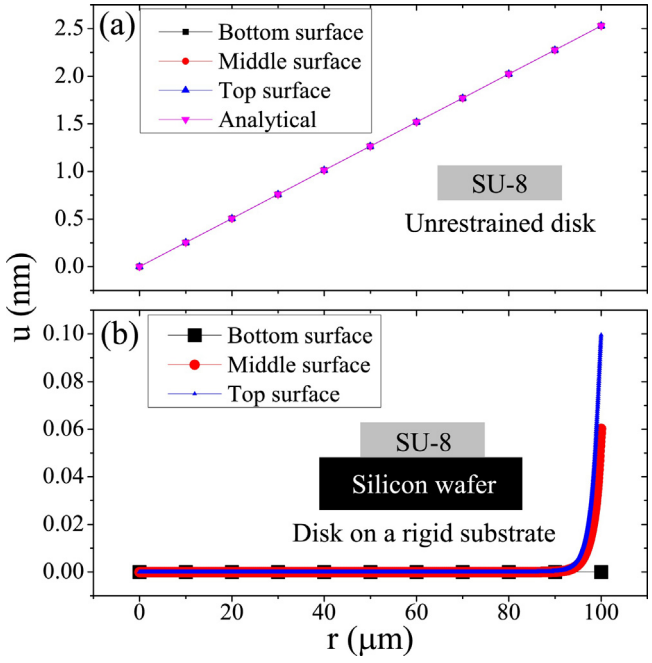

Fig. 2. FEM simulations for two cases of microdisk microresonator deformation. (a) Free-standing (unrestrained) disk. (b) Disk with infinitely rigid support. The displacement values are given as a function of radial distance.

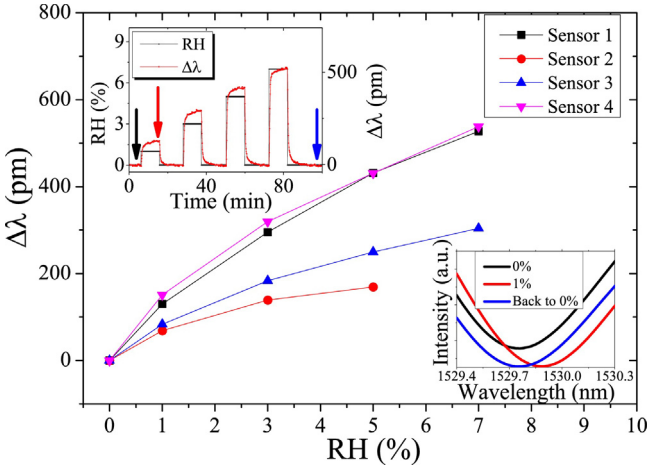

Fig. 3. Resonance shifts of four microdisk sensors under different RH levels. The inset at the top shows an exemplary raw data which belongs to Sensor 1. The zero level base line of the sensor is well preserved. The inset at the bottom shows a WGM resonance for 0%, 1% and again 0% RH. Intensity shift observed between black and blue spectra is attributed to change in coupling efficiency due to drift between the excitation fiber and the waveguide over long time scales. Individual times showing the recording times of these spectra are indicated by the arrows in the inset at the top. Black, red and blue arrows at the top inset represent three cases plotted in the bottom inset, 0%, 1% and again 0% RH, respectively.

chamber. After the N_2 atmosphere with 1% RH is introduced, the resonance wavelength is gradually red shifted by 130 pm after waiting for approximately 6.5 min (see top inset in Fig. 3). Corresponding red shifts are observed for other indicated RH values. For Sensor 1, the resonance wavelength shift versus RH is plotted in the inset of Fig. 3 which shows that the sensor fully recovers to the base line (initial resonance wavelength) after cleaning it with pure N_2. Increasing RH eventually results in a nonlinear behavior in the sensor response. In Fig. 3, the resonance shifts of Sensors 1 to 4 upon the RH change from 0 to 1% are 130, 69, 83, and 151 pm, respectively (on average 108 pm). The different sensitivities are mainly attributed to local variations in the polymer structure in the regions where WGMs are located in a microdisk [27]. In addition, SU-8 thickness variations on the wafer affect the sensitivity of the sensors, since sensitivity usually increases with decreasing thickness [28]. The uncertainty in the wavelength measurement is determined to be <3 pm by calculating the standard deviation at each interval of 0% RH in the raw data given as an inset to Fig. 3. This indicates a limit of detection better than 0.03% RH, assuming linear dependence of the wavelength shift on RH between 0 and 1% RH.

Fig. 4 depicts the response of our sensors during a complete cycle of adjustment of environmental RH. The RH is gradually varied from 0% to 7% and then from 7% back to 0%. A sample raw data taken from Sensor 1 is given as an inset in Fig. 4. The zero level base line of the sensor is very well preserved, but a small deviation is visible between the increasing humidity and decreasing humidity cases, which leads to hysteresis. We define the average hysteresis as the average difference between $\Delta\lambda$ values observed in forward ($\Delta\lambda_{forw}$) and backward directions ($\Delta\lambda_{back}$), normalized to $\Delta\lambda_{forw}$. For the four sensors shown in Fig. 4, average hysteresis is determined as 17% when the data points corresponding to RH values of 1, 3, and 5% are considered. The origins of this hysteresis could be related to slow desorption of water molecules from SU-8 polymer. Depending on the active material, WGM humidity sensors have been reported with [15] and without [14] hysteresis. Another cause of the observed hysteresis can be environmental fluctuations (mainly temperature fluctuations) over long time scales. Such fluctuations can be eliminated by monitoring spectral shifts from a reference sensor device which is kept under ambient conditions at all times.

Response and recovery times of the sensors calculated from the data shown in the top inset of Fig. 3 are depicted in Fig. 5.

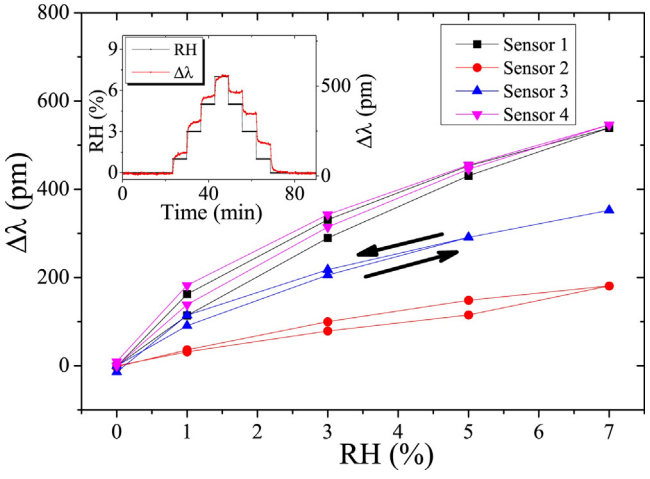

Fig. 4. Hysteresis of the response curves obtained from four microdisk sensors. For all sensors, resonance shift during increasing humidity is less than that of decreasing humidity, as indicated by the arrows. The inset shows an exemplary raw data which belongs to Sensor 1.

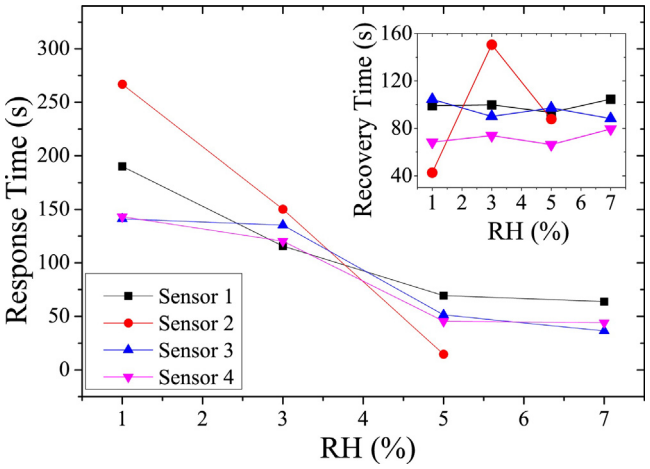

Fig. 5. Calculated response times of four microdisk sensors. Response time decreases as the RH increases, but saturates around 50 s when 5% RH is exceeded. Recovery time is given in the inset. It is approximately constant at 80 s throughout the whole RH range.

Response time is defined as the time it takes for the sensing signal to reach 90% of its final value when the RH is increased from 0% to the target value, whereas the recovery time is the required time for the sensing signal to go down to 10% of its initial value while the water vapor is being removed from the environment. Response time decreases as the RH level increases up to 5% and then saturates around 50 s. This is attributed to the different water ab/adsorption kinetics in or on the SU-8 polymer film when low or high RH is introduced into the environment. The water molecules can adsorb on the surface of the SU-8 polymer layer-by-layer, or diffuse / be absorbed in the SU-8 polymer. On the other hand, the recovery time is approximately constant and independent of RH. This is attributed to the constant dry N_2 flow for removal of the condensed water from SU-8. Although the apparent measured response and recovery times are 50 s and 80 s respectively, actual response and recovery times are expected to be much faster because of the following reasons. Firstly, there is a time delay when the RH level is set to a certain value because of the response of gas flow controllers. Secondly, the finite volumes of the gas chamber and the tubing between the bubbler and the gas chamber delay the introduction of RH to the sensor chip. Finally, each wavelength scan of the laser takes about 8 s to complete, which increases the uncertainty in calculating the response and recovery times. In order to further decrease the response and recovery times, thinner SU-8 layers can be used [13–15,29]. For this purpose, SU-8 microring microresonators can also be employed because microring geometry allows adsorption and desorption from a larger surface area as compared to the microdisk geometry.

Fig. 6 shows repeatability and long term stability of Sensor 1. The sensor is tested under dynamic adsorption–desorption cycles between 0 and 3% RH. It shows an excellent sensing repeatability over 9 cycles since the resonance shift fluctuates between 334 and 340 pm (see Fig. 6(a)). Hence, we conclude that the repeatability in the wavelength measurement is <±1%. To explore long-term stability, another set of such on-off cycles is performed 45 days after the first set, again on Sensor 1 (See Fig. 6(b)). During these 45 days, the sensor is kept under ambient conditions. In 45 days, the sensing response varies between 317 and 322 pm.

SU-8 microdisk microresonators are also tested under high RH conditions. These experiments are summarized in Fig. 7. For Sensor 5, the zero level is conserved after more than 2 hours of exposure to water vapor, even with RH levels up to 50%. The inset to Fig. 7 depicts the shift of WGM resonant wavelength with respect to RH, in which a nonlinear relation is observed. The curve

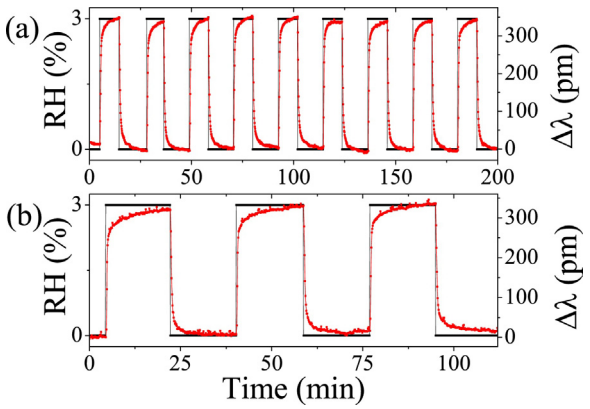

Fig. 6. (a) Multiple cycles of humidity on-off experiments on Sensor 1. (b) A second set of on-off cycles 45 days after the first set of cycles. Both long term and short experiments show good repeatability.

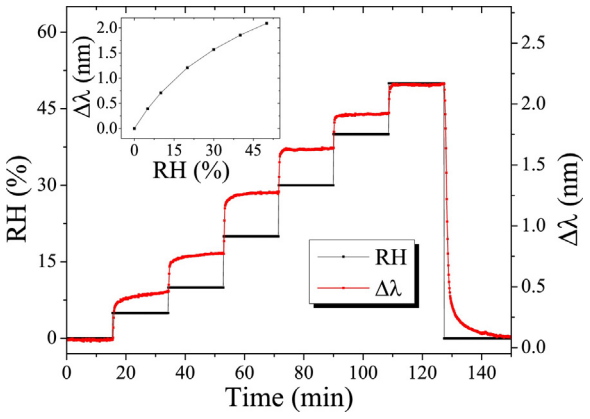

Fig. 7. Response of Sensor 5 to higher RH levels. A third-degree polynomial fits the curve given in the inset.

given in the inset is fitted by a third-degree polynomial equation ($\Delta\lambda(pm) = 0.0093RH^3 - 1.2695RH^2 + 82.08RH + 4.8462$) with correlation coefficient $R^2 = 1$. These measurements indicate that, despite a drop in sensitivity from 78.4 pm/% RH between 0 and 5%RH to 23.5 pm/% RH between 45 and 50%RH, good sensor performance is still preserved at high RH levels. We note that, nonlinear dependence of $\Delta\lambda$ to RH at low RH values between 0 and 7% (observed in Figs. 3 and 4) is not visible in Fig. 7 due to the lack of data points.

6. Conclusion

An optical sensor for measuring environmental RH based on microdisk microresonators fabricated from SU-8 polymer is presented. FEM simulations are performed to analyze the dominant effect on the WGM resonance shift. Refractive index effect is found to be two orders of magnitude higher than the radius change effect. Average sensitivity in the 0–1% RH range is 108 pm/% RH, and the uncertainty in the wavelength measurement is <3 pm. These values imply that the detection limit is better than 0.03% RH. Hysteresis measurements between 0 and 7% RH revealed an average hysteresis of 17%. Repeatability of the sensor is determined to be <±1%. Recovery time of the sensors is constant at ~80 s over different RH levels, but response time decreases and saturates at ~50 s as RH increases. Thinner SU-8 layers or SU-8 microring microresonators instead of microdisk microresonators can be employed to further decrease the response and recovery times. Detection limit of our sensor can be further increased by the use of a second reference sensor device kept under ambient conditions. Spectral drifts observed in the reference sensor due to temperature fluctuations in the environment can be used to correct for the spectral drifts of the actual sensor device. This is the first demonstration of humidity sensing by using SU-8 microdisk and waveguide geometry. This work can lead to sensitive humidity detection at low RH values without requiring complicated microfabrication techniques.

Acknowledgements

We acknowledge financial support from TÜBİTAK (grant no. 110T803 and 115F446) and thank Alexandr Jonáš for proofreading the manuscript.

References

[1] T.A. Kolpakov, N.T. Gordon, C. Mou, K. Zhou, Toward a new generation of photonic humidity sensors, Sensors 14 (2014) 3986–4013.
[2] A. Tripathy, S. Pramanik, J. Cho, J. Santosh, N.A.A. Osman, Role of morphological structure, doping, and coating of different materials in the sensing characteristics of humidity sensors, Sensors 14 (2014) 16343–16422.
[3] Z. Chen, C. Lu, Humidity sensors: a review of materials and mechanisms, Sens. Lett. 23 (2005) 274–295.
[4] A. Rivadeneyra, J.F. Salmerón, M. Agudo-Acemel, J.A. López-Villanueva, L.F. Capitan-Vallvey, A.J. Palma, Printed electrodes structures as capacitive humidity sensors: a comparison, Sens. Actuators A 244 (2016) 56–65.
[5] D.-I. Lim, J.-R. Cha, M.-S. Gong, Preparation of flexible resistive micro-humidity sensors and their humidity-sensing properties, Sens. Actuators B 183 (2013) 574–582.
[6] K. Sager, A. Schroth, A. Nakladal, G. Gerlach, Humidity-dependent mechanical properties of polyimide films and their use for IC-compatible humidity sensors, Sens. Actuators A 53 (1996) 330–334.
[7] S. Fanget, S. Hentz, P. Puget, J. Arcamone, M. Matheron, E. Colinet, P. Andreucci, L. Duraffourg, E. Myers, M.L. Roukes, Gas sensors based on gravimetric detection – a review, Sens. Actuators B 160 (2011) 804–821.
[8] S. Sikarwar, B.C. Yadav, Opto-electronic humidity sensor: a review, Sens. Actuators A 233 (2015) 54–70.
[9] Z.M. Rittersma, Recent achievements in miniaturised humidity sensors – a review of transduction techniques, Sens. Actuators A 96 (2002) 196–210.
[10] C.-Y. Lee, G.-B. Lee, Humidity sensors: a review, Sens. Lett. 3 (2004) 1–14.
[11] K.J. Vahala, Optical microcavities, Nature 424 (2003) 839.
[12] V.S. Ilchenko, A.B. Matsko, Optical resonators with whispering-gallery modes – Part II: Applications, IEEE J. Select. Topics Quant. Electr. 12 (2006) 15.
[13] Q. Ma, L. Huang, Z. Guo, T. Rossmann, Spectral shift response of optical whispering-gallery modes due to water vapor adsorption and desorption, Meas. Sci. Technol. 21 (2010) 115206.
[14] B. Bhola, P. Nosovitskiy, H. Mahalingam, W.H. Steier, Sol–gel-based integrated optical microring resonator humidity sensor, IEEE Sens. 9 (2009) 740–747.
[15] S. Mehrabani, P. Kwong, M. Gupta, A.M. Armani, Hybrid microcavity humidity sensor, Appl. Phys. Lett. 102 (2013) 241101.
[16] J. Zhang, J. Zhong, Y.F. Fang, J. Wang, G.S. Huang, X.G. Cui, Y.F. Mei, Roll up polymer/oxide/polymer nanomembranes as a hybrid optical microcavity for humidity sensing, Nanoscale 6 (2014) 13646–13650.
[17] Y. Wu, T. Zhang, Y. Rao, Y. Gong, Miniature interferometric humidity sensors based on silica/polymer microfiber knot resonators, Sens. Actuators B 155 (2011) 258–263.
[18] D. Dai, L. Yang, Z. Sheng, B. Yang, S. He, Compact microring resonator with 2×2 tapered multimode interference couplers, J. Lightw. Technol. 27 (2009) 4878–4883.
[19] See http://www.microchem.com/Appl-IIIVs-Waveguides.htm (accessed 20.04.16).
[20] J. Zhang, K.L. Tan, H.Q. Gong, Characterization of the polymerization of su-8 photoresist and its applications in micro-electro-mechanical systems (MEMS), Polym. Test. 20 (2001) 693–701.
[21] S. Schmid, S. Kühne, C. Hierold, Influence of air humidity on polymeric microresonators, J. Micromech. Microeng. 19 (2009) 1–9.
[22] A. Felipe, G. Espíndola, H.J. Kalinowski, J.A.S. Lima, A.S. Paterno, Stepwise fabrication of arbitrary fiber optic tapers, Opt. Express 20 (2012) 19893–19904.
[23] J. Lv, Y. Cheng, W. Yuan, X. Hao, F. Chen, Three-dimensional femtosecond laser fabrication of waveguide beam splitters in $LiNbO_3$ crystal, Opt. Mater. Expr. 5 (2015) 1274–1280.
[24] S.-Y. Cho, N.M. Jokerst, A polymer microdisk photonic sensor integrated onto silicon, IEEE Photonics Technol. Lett. 18 (2006) 2096–2098.
[25] M. Eryürek, Y. Karadag, N. Taşaltın, N. Kılınç, A. Kiraz, Optical sensor for hydrogen gas based on a palladium-coated polymer microresonator, Sens. Actuators B 212 (2015) 78–83.
[26] D.R. Southworth, L.M. Bellan, Y. Linzon, H.G. Craighead, J.M. Parpia, Stress-based vapor sensing using resonant microbridges, Appl. Phys. Lett. 96 (2010) 163503.

[27] B.H. Ong, X. Yuan, S. Tao, S.C. Tjin, Photothermally enabled lithography for refractive-index modulation in su-8 photoresist, Opt. Lett. 31 (10) (2006) 1367–1369.
[28] M. Ghadiry, M. Gholami, C.K. Lai, H. Ahmad, W.Y. Chong, Ultra-sensitive humidity sensor based on optical properties of graphene oxide and nano-anatase tio_2, PLOS ONE (2016) 1–14.
[29] G. Rajan, Y.M. Noor, B. Liu, E. Ambikairaja, D.J. Webb, G.-D. Peng, A fast response intrinsic humidity sensor based on an etched singlemode polymer fiber bragg grating, Sens. Actuators A 203 (2013) 107–111.

Biographies

Mustafa Eryürek was born in Razgrad, Bulgaria in 1987. He received his B.Sc. degree from Bilkent University, Physics Department in 2010 and his M.Sc. degree from Koç University, Optoelectronics and Photonics Engineering Program in 2013. He is currently pursuing his Ph.D. in Koç University, Physics Department.

Zuhal Tasdemir received B.S. degrees in both materials science engineering and mechanical engineering from Marmara University, Istanbul, Turkey in 2007 and 2008 respectively. Later, she completed her M.S. degree in materials science engineering from Sabanci University, Istanbul, Turkey in 2009 and her Ph.D. degree in mechanical engineering from Koc University in 2015. During her PhD study, she received the Swiss Government Excellence Scholarship for Foreign Scholars and Artists in 2013 and visited École Polytechnique Fédérale de Lausanne (EPFL), Switzerland. During her stay there, she initiated great collaborations with several groups at EPFL and initiated a joint research proposal with EPFL and the Swiss Federal Laboratories, EMPA. Currently, she is working towards becoming an excellent researcher in the field. Her research interests include micro/ nano fabrication of novel MEMS devices, electrical-mechanical characterization, and finite element modeling of these functional devices.

Yasin Karadag received his B.Sc. (2007) in physics from Bilkent University. He received his M.Sc. (2009) and Ph.D. degrees (2013) in physics from Koç University. In 2013, he joined TUBITAK BILGEM as a senior researcher where he worked on development of high power lasers. Since 2014, he has been an assistant professor at Marmara University, Physics Department. His research interests are optofluidics and tapered fiber spectroscopy.

Suman Anand is a Tubitak research Fellow at Optofluidic and Nano-Optics research laboratory Group of the Physics Division at Koç University. She earned her PhD from Banaras Hindu University (BHU) in 1999. Before this, she was a Leverhulme Fellow at Dundee University, UK. Her current research interest is mainly on Optical tweezers, aerosols, WGMs, droplet resonator and lasing.

Necmettin Kilinc works as an associate professor at Mechatronics Engineering Department, Nigde University, Nigde, Turkey. He received the B.Sc. degree from Marmara University, Istanbul, in 2003, and M.Sc. and Ph.D. degrees from Gebze Technical University in 2006 and in 2012, all in Physics. He has been a research assistant at the Department of Physics Gebze Technical University. After his Ph.D., he started to post doc at Optical Microsystems Laboratory Koc University to research cantilever based biosensors. His research interests are fabrication of nanostructures and thin films of metal oxides and organic materials and structural and electrical properties of these materials and using these materials for bio-chemical sensor applications.

B. Erdem Alaca received the B.S. degree in mechanical engineering from Bogaziçi University, Istanbul, Turkey, in 1997, and the M.S. and Ph.D. degrees in mechanical engineering from the University of Illinois at Urbana-Champaign in 1999 and 2003, respectively. He is currently an Associate Professor in the Department of Mechanical Engineering at Koç University, where he manages Mechanical Characterization and Microfabrication facilities. His research interests include small-scale mechanical behavior and testing of materials and nanowire-based devices. Prof. Alaca is a member of the Turkish National Committee on Theoretical and Applied Mechanics and the Institute of Electrical and Electronics Engineers (IEEE). He was a recipient of the 2009 Distinguished Young Scientist Award from the Turkish Academy of Sciences.

Alper Kiraz is a professor in the physics and electrical-electronics engineering departments at Koç University. He received his B.S. degree in electrical-electronics engineering from Bilkent University in 1998, M.S. and Ph.D. degrees in electrical and computer engineering from the University of California, Santa Barbara in 2000 and 2002, respectively. Between 2002 and 2004 he worked as a post-doctoral associate at the Institute for Physical Chemistry in the Ludwig-Maximilians University, Munich, and received Alexander von Humboldt fellowship. He joined Koç University in 2004 and became a full professor in 2014. Between 2014 and 2015 he was a visiting professor at the Biomedical Engineering of the University of Michigan, Ann Arbor. His current research interests include optofluidics, single molecule spectroscopy/microscopy, optical manipulation, and biomedical instrumentation. His research team pursues various research projects targeting the development of novel micro-optical devices, optofluidic lab-on-a-chip devices, molecular and gas sensors, optofluidic-based renewable energy solutions, and confocal microscope device concepts. He is a member of SPIE and senior member of OSA.